ARTICLES ON SINGLE-MOLECULE PHYSICS AND CHEMISTRY

Direct measurements of memory effects in single-molecule kinetics

Shilong Yang and Jianshu Cao[a)]
Department of Chemistry, Massachusetts Institute of Technology, Cambridge, Massachusetts 02139

(Received 14 February 2002; accepted 18 September 2002)

Statistics and correlations of single-molecule sequences of modulated reactions are explicitly evaluated in the stochastic rate representation. The memory function, introduced through the Gaussian approximation of the stochastic rate expression, characterizes the correlation in single-molecule rate processes in a formalism similar to the stochastic line shape theory. Within this formalism, the on-time correlation is shown to approximate the memory function of the fluctuating rate at discretized effective time separations. A new measurement, the two-event number density, is proposed as a means to map out the memory function over the complete time range. Confirmed by numerical calculations, these relations quantify dynamic disorder caused by conformational fluctuations and hence are useful for analyzing single-molecule kinetics. © *2002 American Institute of Physics.* [DOI: 10.1063/1.1521155]

I. INTRODUCTION

Single-molecule spectroscopy allows us to observe real-time single-molecule trajectories, which consist of a chain of correlated reaction events of various lifetimes and contain rich information about microscopic mechanisms.[1–7] An advantage of single-molecule techniques is the direct observation of variations in reaction kinetics, which are often limited by the spectral resolution in conventional bulk experiments.[8–15] In single-molecule experiments, the observed molecular system interconverts between the dark and bright states so that the fluorescence turns on and off intermittently. The on/off waiting time corresponds to the duration that a single molecule spends in the bright/dark state, and a trajectory of on–off events records the history of the single reactive system. Since only the bright state is monitored through fluorescence emission, conformational dynamics is not directly accessible, and dynamic disorder is a *hidden* mechanism that requires statistical analysis of single-molecule reaction events.[10–12,16–21] In a recent calculation of the two-conformational-channel model, we observed the crossing behavior (i.e., the focal time) in the single-event distribution function and the recurrent behavior (i.e., the echo time) in the two-event distribution function.[18] Many issues remain to be addressed, such as the generality of the two-event echo, the quantitative description of conformational fluctuations in single-molecule kinetics, and the plausibility of direct measurements of memory effects from on–off sequences. In this paper, we use the stochastic rate model to derive explicit expressions for the reported event-averaged quantities and introduce two quantitative measurements of the memory function.

The kinetics considered here is more complicated than direct single-molecule measurements of conformational fluctuations. Using single-molecule fluorescence resonant energy transfer (FRET), Edman *et al.* and Jia *et al.* studied lifetimes of a TMR fluorophore attached to biomolecules and found double exponential decays.[4,5] Geva and Skinner analyzed these measurements[10] and successfully extracted the interconversion rate between the conformational states. The FRET experiments and the subsequence analysis are based on the fact that the FRET rate is much faster than conformational relaxation so that the lifetime of a single event is dictated by the transient conformation. In fact, the average lifetimes of the two channels are so disparate in these experiments that one can assign a decay event to a conformational channel and thus directly monitor the interconversion between the two channels. As shown in Appendix A and in a recent paper, single-molecule FRET signals are better expressed as an inhomogeneous average over transient configurations. The interpretation of single-molecule kinetics is less obvious when the average lifetimes are not so disparate and the conformational fluctuation rate is comparable to the decay rate. This complication arises when the decay process has a competing time scale such as the environmental time scale. Wolynes and co-workers have explored the possibility of using intermittency to extract information about conformational effects from single-molecule sequences.[12,13,22] An important example of single-molecule kinetics is the single-molecule enzymatic turnover experiment by Lu, Sun, and Xie.[16] Analyzing single-molecule reaction sequences, these authors demonstrated slow fluctuations in the turn-over rate of cholesterol oxidation and the dependence of enzymatic turnovers on previous events. Another interesting example is the fluorescence characteristics of single dye molecules adsorbed on a glass surface. Weston *et al.*[11] proposed that the emission spectrum and efficiency are modulated by the interconversion between two ground state potential minima. The purpose of this paper is to quantify single-molecule data

[a)]Electronic mail: jianshu@mit.edu

analysis in a unified framework and to propose more effective measurements of memory effects.

Single reaction events are often modulated by conformational distribution and fluctuations which cannot be described by conventional chemical kinetics. Phenomenological chemical kinetics quantify a first-order rate process with the equilibrium constant measured by the ratio of equilibrium reactant and product concentrations, and with the total rate constant obtained from exponential relaxation to the equilibrium configuration. The phenomenological chemical reaction is a Poisson process, reaction events are stochastically independent, and the nonequilibrium concentration decays exponentially. In a realistic situation, the decay rate is not a constant but modulated by the evolving conformational configuration. (Solvent interactions, intramolecular couplings, electrostatic potentials, geometric effects of macromolecules, etc.)[23–29] Single-molecule experiments monitor rate fluctuations occurring during single decay events, which cannot be easily detected using ensemble-averaged experimental techniques. In Sec. II, we introduce the modulated reaction model as the generic scheme to incorporate effects of environmental modulation on rate processes, and define related single-molecule quantities to elucidate the difference between single-molecule and ensemble averaged measurements.

Single-molecule sequences can be analyzed with several methods,[2] including fluorescence intensity correlation function, on-time histogram, joint probability of two on-time events, on-time correlation function, etc. It is not clear how to relate these different quantities and how to quantify modulation effects on reactions. In Sec. VI, we introduce a different but equivalent representation of modulated reactions: the stochastic rate model, where the evolution of the time-dependent rate is treated as a stochastic process. Similar to Kubo–Anderson's stochastic rate theory,[30,31] the stochastic process of the rate is described by the average rate, used in conventional chemical kinetics, and the memory function, which characterizes memory effects due to the coupling of the reaction to its environments. As a result, all single-molecule quantities can be explicitly evaluated in terms of the average rate and the memory function. As shown in Sec. III A, the memory function directly gives the interconversion rate for the two-channel model, but cannot be decomposed into reaction and modulation factors for a multiple-channel model. In general, the memory function is a convolution of reactions and conformational fluctuations, but decays asymptotically to the fundamental mode of conformational relaxation. With these developments in Sec. III, we can express single-molecule measurements in terms of the memory function (e.g., the two-event echo in Appendix B) and model experimental observations of stretched exponential and power-law decay.

In Sec. IV, we establish the relation between the memory function and the on-time correlation function. With the stochastic rate formalism, we should distinguish two stochastic quantities of different nature: the on-state waiting time dictated by the time-dependent rate and the reaction rate dictated by the conformational dynamics. Thus, we observe a short decay event from a slow channel and a long decay event from a fast channel. It is also possible that because of conformational changes the system which enters the bright state from the slow channel may react from the fast channel. Instead of associating an on-state event with a specific conformational channel, we correlate two on-time events to reveal the correlation hidden under stochastic fluctuations. There are two ways to register the on-time correlation as a function of the number of events in between, or as a function of the time separation. The first kind of on-time correlation function is the focus of our discussion. It has the advantage of having an equal number of data points for different separations of events and the disadvantage of using discretized variables. It is shown in Sec. IV that the on-time correlation function is equal to the memory function evaluated at the average time separation between two on-time events. This approximate relation is proved under two conditions: the Gaussian limit, where the second cumulant contribution is much smaller than the constant rate term, and the slow modulation limit, where conformational fluctuation time scale is much slower than the reaction process time scale. The second kind of on-time correlation function is discussed in Appendix C and is related to the two-event number density discussed in the following.

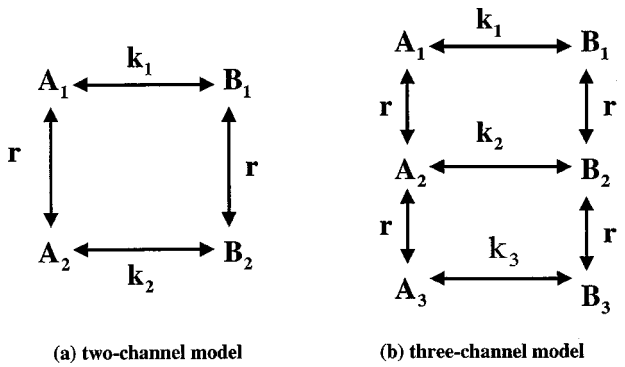

FIG. 1. An illustration of (a) the two-channel model and (b) the linear three-channel model.

In Sec. V, we introduce a new single-molecule measurement: the two-event number density. Along single-molecule kinetics sequences, the decay events are evenly and randomly distributed, so the number density of events is a constant. Now let us take two events along a sequence and register the two events with the time separation from the beginning of one event to the end of another event. Are two events randomly distributed? Yes, if the reaction events are not correlated, the two-event number density is a constant. In the presence of memory, events of similar lengths are likely to group, so that the deviation from the constant number density is a new measure of memory effects. We can show that the deviation from the constant number density is exactly proportional to the memory function for a reaction with infinite fast backreaction rate, and is approximately proportional to the memory function for a general reaction. In comparison, the on-time correlation functions are recorded at discretized time separations and are thus less accurate, while the two-event number density are recorded continuously and are thus more reliable. Our main results are confirmed by nu-

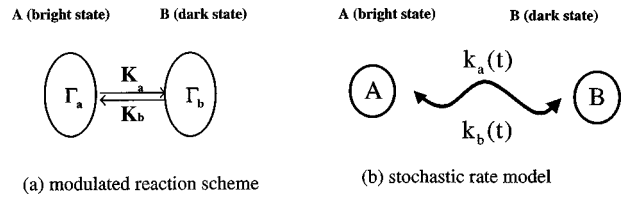

FIG. 2. An illustration of (a) the modulated reaction scheme and (b) the stochastic rate model.

merical simulations in Secs. IV and V, and are summarized in Sec. VI.

II. MODULATED REACTION MODEL

The influence of conformational fluctuations on chemical kinetics is described by the modulated reaction model illustrated in Figs. 1 and 2(a).[17–20,23,29,32,33] In this model, the reaction rate constant depends on environments which are represented by conformational channels, and different channels interconvert according to conformational dynamics. The conformational channels refer to complex environments that influence the reaction process, and arise from various molecular mechanisms including intramolecular structures, intermolecular interactions, solvent configurations, etc. Two specific examples of the generic modulated model, the two-channel model and the three-channel model, are illustrated in Fig. 1 and will be used later in explicit calculations. Modulated reaction model has been extended to the analysis of single-molecule quantum waiting time distribution functions[14,22,34,35] and heterogeneous diffusion process.[36–41] The kinetics of the generic modulated reaction model follows:

$$\begin{pmatrix} \dot{\rho}_a(t) \\ \dot{\rho}_b(t) \end{pmatrix} = -\begin{pmatrix} \Gamma_a + K_a & -K_b \\ -K_a & \Gamma_b + K_b \end{pmatrix} \begin{pmatrix} \rho_a(t) \\ \rho_b(t) \end{pmatrix}, \tag{1}$$

where Γ_a governs the conformational dynamics in the bright state A (i.e., the on-state), Γ_b governs the conformational dynamics in the dark state B (i.e., the off-state), K_a is the forward rate from the bright state to the dark state, and K_b is the backward rate from the dark state to the bright state. For a multiple channel model with a discretized distribution of conformational channels, ρ is a vector, K and Γ are rate matrices. For a continuous model with a set of conformational coordinates, ρ and K are functions of the conformational coordinates, and Γ is a differential operator which governs the evolution of these coordinates. The modulated reaction model can be regarded as a hidden Markovian scheme, where K dictates the reaction directly and Γ characterizes the hidden mechanism which affects the reaction process indirectly.

Although introduced in the context of single-molecule reactions, the modulated reaction model is general enough to represent a broad class of kinetic processes with dynamic disorder. In complex chemical processes, chemical reactions are usually modulated by geometric constraints, slow structural relaxation, and hydrogen bonding and network in aqueous systems. In the presence of these slow environmental fluctuations, the competition between the reaction dynamics and the conformational dynamics leads to nonexponential kinetics and memory effects.[23–29] In a paper titled "Rate processes with dynamical disorder," [42] Zwanzig listed examples of such processes which include self-diffusion in water, gated diffusion, protein dynamics, fluorescence depolarization, dynamical percolation, barrierless relaxation, etc. Essentially, any sequence composed of two distinct measurements can be mapped to two-state kinetics, where the states refer to chemical states, fluorescence states, charge transfer states, binding sites, different modes of hopping, different regions of diffusion, etc.

The modulated reaction model is discussed in details in Refs. 18 and 21. For convenience of further calculations, we summarize these discussions and elaborate on the physical meanings where necessary.

(1) The reversible full reaction in Eq. (1) can be decomposed into the forward half-reaction described by the survival probability $G_a(t)=\exp[-t(\Gamma_a+K_a)]$ and the backward half-reaction by the survival probability $G_b(t)=\exp[-t(\Gamma_b+K_b)]$. The Green's function solution to Eq. (1) can be expanded into a series of half-reactions linked by the forward rate constant matrix K_a and the backward rate constant matrix K_b. For example, the bright state Green's function associated with the fluorescence correlation function is equivalent to an infinite series of half-reaction sequences

$$G_{aa} = G_a + G_a \cdot K_b G_b \cdot K_a G_a + G_a \cdot K_b G_b \cdot K_a G_a \cdot K_b G_b \cdot K_a G_a + \cdots, \tag{2}$$

where the dot represents a time convolution. For an ergodic system, the population evolution measured in bulk experiments is equivalent to the summation of all possible sequences of half-reaction events along single-molecule trajectories, and the equilibrium ensemble-averaged quantities in the bulk state can be recovered by averaging along single-molecule trajectories.

(2) The phenomenological rate constant in chemical kinetics can be interpreted as the inverse of the average lifetime at the bright or dark state, giving

$$\bar{t}_a = \int_0^\infty \sum G_a(t) F_a dt = \frac{\Sigma \rho_a}{\Sigma K_a \rho_a} = \frac{1}{k_a} \tag{3}$$

and, similarly, $\bar{t}_b = 1/k_b$. In Eq. (3), F_a is the stationary flux defined in Eq. (6). Evidently, the macroscopic rate constant in phenomenological chemical kinetics is simply an inhomogeneous average of the microscopic reaction rate constants and therefore does not contain any information about dynamic disorder. The ratio of the average forward and backward reaction rate constants satisfies the phenomenological detailed balance relation

$$k_a n_a = k_b n_b, \tag{4}$$

where $n_a = \Sigma \rho_a$ and $n_b = \Sigma \rho_b$ are, respectively, the total equilibrium populations in the bright state and in the dark state. In the context of single-molecule measurements, the detailed balance relation in Eq. (4) is a result of the long-time averaging of the waiting time along single-molecule trajectories, which defines both the average rate constant and the equilibrium distribution. Furthermore, bulk-state relaxation experiments measure the total rate constant $k_{\text{total}} = k_a$

$+k_b$, whereas the forward and backward rate constants are obtained through the detailed balance condition in Eq. (4). In contrast, single-molecule experiments separate the forward and backward half-reactions, and determine the two rate constants from the average on and off times.

(3) The time-independent solution to Eq. (1) defines the equilibrium distribution, $(\Gamma_a+K_a)\rho_a=K_b\rho_b$ and $(\Gamma_b+K_b)\rho_b=K_b\rho_a$, which relate ρ_a to ρ_b and vice versa. Taking the trace of both sides of the two equations, we obtain the macroscopic detailed balance relationship, $n_a k_a=n_b k_b$. The overall balance condition follows directly from the conservation of the flux, but it does not exclude the possibility of a net current circulating around conformational channels. In fact, this kind of net current can lead to the intriguing phenomenon of Brownian ratchets. For example, different modes of diffusion lead to a net motion driven by the coupling of random Brownian motions and chemical reactions. The possibility of a net current can be excluded by equating the microscopic fluxes of the forward and backward reactions

$$K_a\rho_a=K_b\rho_b, \tag{5}$$

which leads to the equilibrium conformational distribution $\Gamma_a\rho_a=\Gamma_b\rho_b$. With the same conformational dynamics for the two states, $\Gamma_a=\Gamma_b$, we have $\rho_a\propto\rho_b$ and $K_a\propto K_b$, which are useful for further calculations.

(4) To formulate event-averaged quantities, it is necessary to introduce the stationary occurrence probability flux

$$\begin{pmatrix} F_a \\ F_b \end{pmatrix}=\mathcal{N}\begin{pmatrix} K_b\rho_b \\ K_a\rho_a \end{pmatrix}, \tag{6}$$

where F_a is the stationary flux from the bright state to the dark state, and F_b is the stationary flux from the dark state to the bright state. It follows that $\Sigma K_a\rho_a=\Sigma K_b\rho_b=\mathcal{N}^{-1}$, implying the conservation of the flux.[18] Given the stationary fluxes, we define the distribution function of on-time events as $f_a(t)=\Sigma K_a G_a(t)F_a$ and the joint distribution function of on-off events as $f_{ab}(t_2,t_1)=\Sigma K_b G_b(t_2)K_a G_a(t_1)F_a$, which will be evaluated explicitly. These event-averaged quantities cannot be obtained directly from bulk experiments and must be collected along single-molecule trajectories.

III. STOCHASTIC RATE MODEL

As demonstrated in Ref. 21, given a specific model, the single-molecule quantities can be computed and the features such as the focal time and the echo time can be identified. In this paper, we will show the generality of these features by virtue of the stochastic rate model. The environmental fluctuations introduces a time dependence on the rate constant, which can now be treated as a stochastic variable. Similar to Kubo's stochastic line-shape theory,[30,31] each realization of the stochastic rate defines a rate process, and single molecular measurements can be obtained by taking a stochastic average of rate fluctuations. The modulated reaction model is analogous to the Schrödinger picture in quantum mechanics, as the occupancy in each conformational channel changes with time but the rate constant for each channel remains constant. The stochastic reaction rate model is analogous to the Heisenberg picture in quantum mechanics, as the rate evolves with time. As illustrated in Fig. 2, though in different pictures, these two models are equivalent.

To begin, we write the kinetics of the generic modulated reaction model in a compact form

$$\dot{\rho}(t)=-(\Gamma+K)\rho(t), \tag{7}$$

where Γ characterizes the conformational dynamics and K characterizes the reaction kinetics. In general, Γ can be any dynamic operator [e.g., $\Gamma=-\lambda\theta\partial_x(\partial_x+x/\theta)$ is the Fokker–Planck operator for normal diffusion in a harmonic potential], and K can be any form of kinetic processes, including discretized multichannel rate and coordinate-dependent rate. We introduce the stochastic representation for modulated reactions by rewriting the Green's function solution to Eq. (7) in the interaction picture as

$$G(t)=e^{-(\Gamma+K)t}=e^{-\Gamma t}\exp\left(-\int_0^t K(\tau)d\tau\right). \tag{8}$$

The time-dependent rate is defined through a matrix transformation $K(t)=e^{\Gamma t}Ke^{-\Gamma t}$ so that conformational modulation is incorporated into the time dependence of the rate.

With the time-dependence rate, all single-molecule quantities can be evaluated explicitly in the stochastic rate model. For example, using the identity $\Sigma\Gamma_a=0$, the average survival probability in the bright state can be written as $S(t)=\langle G_a(t)\rangle=\langle\exp(-\int_0^t K_a(\tau)d\tau)\rangle$, where the average is taken with respect to the equilibrium conformational distribution $\langle A\rangle=\Sigma A\rho_a/\Sigma\rho_a$. Cumulant expansion of $S(t)$ leads to

$$S(t)=\exp\left[\sum_{n=1}^{\infty}\frac{(-1)^n}{n!}\int_0^t d\tau_1\cdots\int_0^t d\tau_n\chi_n(\tau_1,\ldots,\tau_n)\right], \tag{9}$$

where $\chi_n(\tau_1,\ldots,\tau_n)$ is the nth order cumulant function. As a result of the detailed balance condition, $\Gamma_a\rho_a=0$, the average rate and correlation functions are stationary. Thus, we have

$$\chi_1(t)=\langle K_a(t)\rangle=\langle K_a\rangle=k_a, \tag{10}$$

which is the phenomenological rate constant, and

$$\chi_2(t_1,t_2)=\langle\delta K_a(t_1)\delta K_a(t_2)\rangle=\langle\delta K_a e^{-\Gamma_a(t_1-t_2)}\delta K_a\rangle=\chi_{aa}(t_1-t_2), \tag{11}$$

which rigorously defines the memory function for the stochastic rate. The initial value of the memory function gives the variance of the reactive rate $\chi(0)=\langle\delta k^2\rangle=k_d^2$. By truncating the expansion in Eq. (9) to second order, we obtain the Gaussian stochastic rate model

$$S(t)=\exp[-k_a t+M_{aa}(t)] \tag{12}$$

with $M_{aa}(t)=\int_0^t(t-\tau)\chi_{aa}(\tau)d\tau$. Similar expressions can be obtained for the backward half-reaction as well as for the reversible full-reaction. Since the survival probability decreases with time, $k_a\gg\int_0^t(1-\tau/t)\chi_{aa}(\tau)d\tau$ has to be satisfied, which implies a small variance of reaction rates and a finite correlation time for conformational fluctuations. We emphasize that the stochastic model and the memory function are completely general whereas the Gaussian stochastic rate model is approximate.

The kinetic problem considered here is more general than conformational kinetics probed by single-molecule fluorescence resonant energy transfer (FRET) or other related techniques. With these techniques, the decay process is much faster than conformational fluctuations so that the variation of the rate during a single decay event can be ignored. Thus, the single-molecule sequence consists of a large number of forward half-reaction events, where the on-time duration corresponds a specific conformational state, and the evolution of the decay time directly records conformational dynamics. In comparison, for single-molecule kinetics, we have to properly treat the convolution of reaction and modulation, i.e., the time dependence of the rate during a single decay event. Evidently, the reaction limit of our results here will be useful for analyzing FRET. In Appendix A, we discuss the statistics and correlation of FRET measurements and show that the memory function remains a useful tool.

The importance of the memory function in single-molecule kinetics can be better appreciated by the comparison with the memory function in condensed phase spectroscopy.[30,31] Stochastic line-shape theory describes stochastic fluctuations of the transition frequency using the energy gap correlation function and thus provides a universal language to unify and quantify different optical spectroscopy measurements. The specific form of the energy gap memory function depends on environmental dynamics and the coupling between the quantum transition and its environment. The evaluation of this phenomenological memory function has motivated microscopic theories of solvation dynamics and solution spectroscopy. In a similar fashion, the introduction of the memory function in this paper provides a unified framework to quantify memory effects in single-molecule kinetics and to explicitly evaluate single-molecule measurements. The memory kernel is the key quantity we extract from single-molecule sequences and use to characterize modulated reactions. For example, in Appendix B, we derive the expression for the two-event distribution function within the framework of the Gaussian stochastic rate approximation. Several forms of the memory function are discussed in the following.

A. Discretized conformational states: Two-channel and multichannel models

The simplest example of modulated reactions is the two-conformational-channel model illustrated in Fig. 1(a) For the forward half-reaction, we have $k_a=\rho_1 k_1+\rho_2 k_2$, $k_d^2=\rho_1\rho_2(k_1-k_2)^2$, and

$$\chi_{aa}(t)=k_d^2\exp[-(\gamma_1+\gamma_2)t], \tag{13}$$

where $\rho_1=\gamma_2/(\gamma_1+\gamma_2)$ and $\rho_2=\gamma_1/(\gamma_1+\gamma_2)$ are the equilibrium populations of the two conformational channels. From the memory function, we will be able to determine the total interconversion rate between the two channels. For a multichannel model, we will not be able to find such a simple interpretation for the memory function except for special cases as in Fig. 1(b). In general, the memory function is a summation of many exponential functions and characterizes the average effects of conformational modulation on the reactive rate process.

B. Continuous conformational states: Coordinate dependence

Our definition of the memory function provides a possible interpretation of the recent finding of stretched exponential relaxation in single-molecule experiments.[43] In a general situation where the rate constant is coupled to a set of conformational degrees of freedom with the coordinate dependence $k(x)$, the memory function becomes

$$\chi(t)=\frac{1}{(2\pi)^2}\int d\zeta_1 d\zeta_2 \tilde{k}(\zeta_1)\tilde{k}(\zeta_2)\{\langle\exp[i\zeta_1 x(0)+i\zeta_2 x(t)]\rangle-\langle\exp[i\zeta_1 x(0)]\rangle\langle\exp[i\zeta_2 x(0)]\rangle\}, \tag{14}$$

where $\tilde{k}(\zeta)=\int k(y)\exp(iy\zeta)dy$ is the Fourier transform of the rate function $k(x)$ and the stochastic average is carried out with respect to the conformational dynamics of $y(t)$. Assuming a Gaussian stochastic process for the conformational coordinate Eq. (14) can be evaluated with the second-order cumulant expansion. This expression incorporates a large class of modulated rate processes and leads to a stretched exponential with a proper choice of the coordinate dependence in the rate function.

C. Long-time behavior

We note that the memory function measures modulating effects of environments on two-state kinetics, but does not directly probe environmental fluctuations. Nevertheless, the asymptotic behavior of the memory function reveals the nature of the long-time relaxation of environmental fluctuations. To demonstrate this, we expand conformational fluctuations as $G(t)=|\varphi_n\rangle E_n(t)\langle\varphi_n|$ where the eigenstates satisfy $\langle\varphi_n|\varphi_m\rangle=\delta_{nm}$, and $E_n(t)$ is the characteristic function for the nth eigenstate. In order words, $\varphi_n(x)$ are the normal modes of conformational fluctuations. In this basis set, we expand the rate constant as $k(x)=\Sigma c_n\varphi_n(x)$ so that $\langle k(x)\rangle=c_0$, and

$$\chi(t)=\sum_{n=1}^{\infty} c_n^2 E_n(t). \tag{15}$$

The smallest nonzero eigenvalue has the slowest decay and thus dominates the asymptotic behavior, i.e.,

$$\lim_{t\to\infty}\chi(t)\propto E_1(t) \tag{16}$$

which directly probes the fundamental mode of conformational fluctuations. As an important example, we demonstrate this aspect of the memory kernel using the example of subdiffusive environments.

D. Memory function for subdiffusive environments

To illustrate the generality of memory effects, we hereby consider a single-molecule experiment in a disordered medium where the conformational dynamics is modeled by subdiffusive motion in a harmonic potential. Subdiffusive transport is widely observed in diverse fields, including charge transport in amorphous semiconductors, Nuclear magnetic

resonance diffusometry in disordered materials, and bead dynamics in polymer networks. Metzler, Barkai, and Klafter proposed a generalized fractional Fokker–Planck equation for anomalous diffusion, and later justified the approach from a continuous time random walk model.[44] Unlike linear Brownian motion in the diffusive regime, the mean square displacement in the free subdiffusive space follows

$$\langle(\Delta x)^2\rangle = \frac{2K_\gamma}{\Gamma(1+\gamma)}t^\gamma \quad \text{with} \quad 0<\gamma<1, \tag{17}$$

where K_γ is the generalized diffusion coefficient, and the Stokes–Einstein relation is generalized as $K_\gamma = k_BT/m\eta_\gamma$, where η_γ is the generalized friction coefficient. The subdiffusive motion in a potential is described by the corresponding Fokker–Planck operator $-\mathcal{L}_{\rm FP} = \partial_x[V'(x)/m\eta_\gamma] + K_\gamma\partial_x^2$. In a harmonic potential, $V(x) = m\omega^2x^2/2$, the Green's function for the subdiffusive motion is

$$G(x,x',t) = \sqrt{\frac{m\omega^2}{2\pi k_BT}}\sum_{n=0}^{\infty}\frac{1}{2^n n!}E_\gamma(-n\tilde{t}^\gamma) \times H_n\left(\frac{\tilde{x}'}{\sqrt{2}}\right)H_n\left(\frac{\tilde{x}}{\sqrt{2}}\right)\exp\left[-\frac{\tilde{x}^2}{2}\right], \tag{18}$$

where the characteristic time unit τ is defined by $\tau^{-\gamma} = \omega^2/\eta_\gamma$, $\tilde{t} = t/\tau$ and $\tilde{x} = x\sqrt{m\omega^2/k_BT}$ are temporal and spatial coordinates in reduced units, $H_n(x) = (-1)^n \times \exp[x^2]\partial_x^n\exp[-x^2]$ is the Hermite polynomial, and $E_\gamma(z) = \Sigma_{m=0}^{\infty} z^m/[\Gamma(1+\gamma m)]$ is the Mittag–Leffler function. For $\gamma = 1$, the Mittag–Leffler function becomes the exponential function, $E_1(z) = \exp(z)$. The equilibrium distribution is deduced from the long time limit of the Green's function, $\rho(x) = \sqrt{m\omega^2/2\pi k_BT}\exp[-\tilde{x}^2/2]$.

In general, a coordinate-dependent rate function can be expanded as $k(x) = \Sigma_{n=0}^{\infty} c_n H_n(\tilde{x}/\sqrt{2})$ so that the average stochastic rate and the correlation function of the stochastic rate become $\langle k(x)\rangle = c_0$ and

$$\chi(t) = \langle \delta k(x)G(x,x',t)\,\delta k(x')\rangle = \sum_{n=1}^{\infty} c_n^2 2^n n! E_\gamma(-n\tilde{t}^\gamma). \tag{19}$$

In the long time limit, the memory function of the fluctuating rate $\chi(t)$ follows a power law decay according to the properties of the Mittag–Leffler function.

As a special case, we assume a quadratic form of the coordinate dependence, i.e., $k(x) = \kappa x^2$, so that the correlation function of the stochastic rate is given by $\chi(t) = \chi(0)E_\gamma(-2\tilde{t}^\gamma)$. In the short time regime, when $t \ll \tau$,

$$E_\gamma(-2\tilde{t}^\gamma) \sim 1 - 2\tilde{t}^\gamma/\Gamma(1+\gamma) \sim \exp[-2\tilde{t}^\gamma/\Gamma(1+\gamma)] \tag{20}$$

is a stretched exponential; while in the long time regime, $t \gg \tau$,

$$E_\gamma(-2\tilde{t}^\gamma) \sim \frac{\tilde{t}^{-\gamma}}{2\Gamma(1-\gamma)} - \frac{\tilde{t}^{-2\gamma}}{4\Gamma(1-2\gamma)} \tag{21}$$

is a power law decay. Numerical calculations of $E_\gamma(-2\tilde{t}^\gamma)$ are shown in Fig. 3 for different values of γ. As γ approaches 1, the Mittag–Leffler function becomes close to a single exponential function; while for small γ, it clearly deviates from exponential decay and shows the power-law behavior in the long time regime.

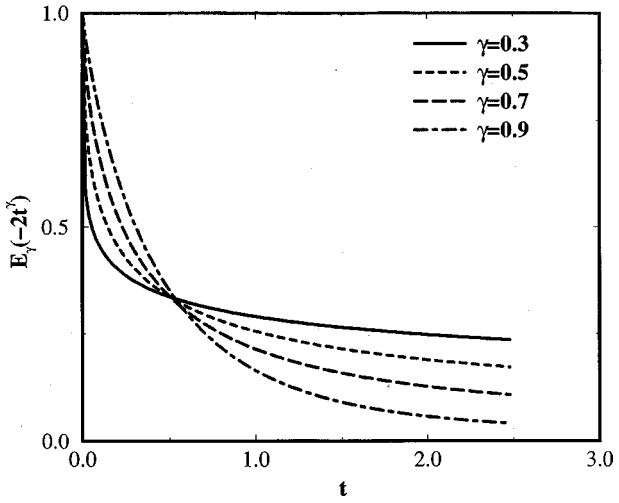

FIG. 3. Numerical calculation of $E_\gamma(-2t^\gamma)$. For γ close to 1, $E_\gamma(-2t^\gamma)$ is similar to exponential decay; while for small γ, it deviates from exponential decay and exhibits stretched exponential in the short time regime and power-law behavior in the long time regime.

IV. ON-TIME CORRELATION FUNCTION

One direct measure of the memory function is the on-time correlation function illustrated in Fig. 4, which was first used in Xie's experiment as a measure of memory effects. With the introduction of the stochastic rate model and memory function, we are now able to explicitly show the relation between the memory function and the on-time correlation function. Here, this relationship is proved within the slow modulation limit and the small variance limit. Though both are derived for the small variance limit, the first proof invokes the second cumulant approximation but does not require the slow modulation assumption; and the second proof does not involve any assumptions about the convergence of the memory function but requires the slow modulation assumption.

A. Second cumulant expansion

The on-time correlation function is defined as

$$\mathrm{Cor}(n) = \frac{\overline{t_1 t_{n+1}} - \overline{t}^2}{\overline{t^2} - \overline{t}^2}, \tag{22}$$

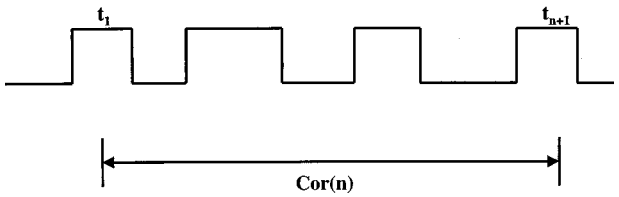

FIG. 4. Two on-time events separated by n off-events along a typical single-molecule trajectory.

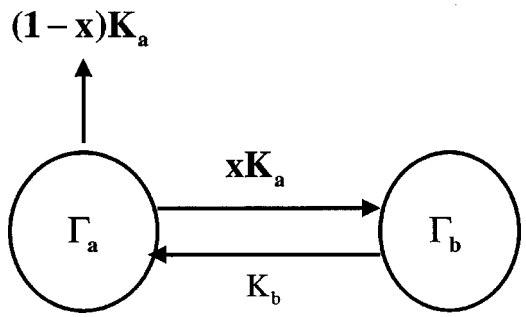

FIG. 5. An illustration of the reaction scheme for the evaluation of the generating function $H(x)$.

which is the cross-correlation function of two on-time events separated by n off-events. From Eq. (5) of Ref. 18, the joint probability distribution is given as

$$f(t_1,t_{n+1})=\sum K_aG_a(t_{n+1})K_b\tilde{G}_b[K_a\tilde{G}_aK_b\tilde{G}_b]^{n-1}\times K_aG_a(t_1)F_a, \tag{23}$$

so that

$$\overline{t_1t_{n+1}}=\int dt_1\int dt_{n+1}f(t_1,t_{n+1})t_1t_{n+1}=\langle[\tilde{G}_aK_a\tilde{G}_bK_a]^n\tilde{G}_a\rangle/k_a \tag{24}$$

with $\tilde{G}=\int_0^\infty G(t)dt$. Here, the stochastic average is defined as $\langle A\rangle=\Sigma A\rho_a/\Sigma\rho_a$. To evaluate the on-time correlation function, we introduce a generating function $H(x)=\Sigma_{n=0}^\infty\overline{t_1t_{n+1}}x^n$, where the $n=0$ term is included for convenience and $x\leqslant 1$ is assumed for convergence. Thus, we have

$$k_aH(x)=\sum_{n=0}x^n\langle[\tilde{G}_aK_b\tilde{G}_bK_a]^n\tilde{G}_a\rangle=\langle\tilde{G}_{aa}(x)\rangle=\int_0^\infty\langle G_{aa}(t,x)\rangle dt, \tag{25}$$

where the resummation similar to Eq. (2) is used. As illustrated in Fig. 5, the Green's function $G_{aa}(t,x)$ corresponds to the following kinetics:

$$\begin{pmatrix}\dot{\rho}_a(t)\\ \dot{\rho}_b(t)\end{pmatrix}=-\begin{pmatrix}\Gamma_a+K_a & -K_b\\ -xK_a & \Gamma_b+K_b\end{pmatrix}\begin{pmatrix}\rho_a(t)\\ \rho_b(t)\end{pmatrix}, \tag{26}$$

which describes the forward reaction with rate xK_a, the backward reaction with rate K_b, and the population depletion at the bright state with rate $(1-x)K_a$. For symmetric reactions with $K_a=K_b=K$, Eq. (26) is solved explicitly for a stochastic rate process $K(t)$, giving

$$\begin{aligned}kH(x)&=\int_0^\infty dt\,\tfrac{1}{2}\left\langle\exp\left(-(1-\sqrt{x})\int_0^tK(\tau)d\tau\right)+\exp\left(-(1+\sqrt{x})\int_0^tK(\tau)d\tau\right)\right\rangle\\&\approx\tfrac{1}{2}\int_0^\infty dt\{\exp[-(1-\sqrt{x})kt+(1-\sqrt{x})^2M(t)]+\exp[-(1+\sqrt{x})kt+(1+\sqrt{x})^2M(t)]\},\end{aligned} \tag{27}$$

where the second cumulant truncation is applied and $M(t)$ is given as $M(t)=\int_0^t\chi(\tau)(t-\tau)d\tau$. Under the small variance condition, Eq. (27) is expanded to the leading order of $M(t)$, giving

$$kH(x)=\int_0^\infty\{[1+M(t)+xM(t)]\cosh(kt\sqrt{x})-2\sqrt{x}M(t)\sinh(kt\sqrt{x})\}e^{-kt}dt. \tag{28}$$

This closed-form expression is then used to generate the moment in order of x^n, leading to $k^2H(x)=\Sigma x^n[1+I_{2n}+I_{2n-2}-2I_{2n-1}]$ where $I_m=\int_0^\infty d\tau M(\tau)(k\tau)^me^{-kt}/m!$. Assuming that the memory function of the rate varies much slower than the rate process, the integral of $M(\tau)$ can be approximated by the value of the first moment $t_m=(m+1)/k$, that is $I_m\approx M(t_m)$. Then, the difference function becomes

$$I_{2n}+I_{2n-2}-2I_{2n-1}\approx M\left(\frac{2n+1}{k}\right)+M\left(\frac{2n-1}{k}\right)-2M\left(\frac{2n}{k}\right)\approx\frac{1}{k^2}\chi\left(\frac{2n}{k}\right), \tag{29}$$

where the continuous limit is taken under the slow relaxation assumption. Combining Eqs. (22)–(29), we finally arrive at an approximate expression

$$\mathrm{Cor}(n)=\frac{\chi(2n/k)}{\chi(0)}=\frac{\chi(t_{\mathrm{eff}})}{\chi(0)}, \tag{30}$$

indicating that the on-time correlation function is proportional to the memory function of the rate at the discrete time separation. The number of off-events in $\mathrm{Cor}(n)$ is translated into the average time separation between two events in $\chi(t)$. For asymmetric reactions, Eq. (30) can be generalized to $\mathrm{Cor}(n)=\chi(n/k_f+n/k_b)/\chi(0)$, with the effective time separation $t_{\mathrm{eff}}=n/k_f+n/k_b$. Although the final result in Eq. (30) is obtained approximately under the slow modulation limit, Eq. (29) is derived without this approximation and is therefore more general.

The generating function in Eq. (25) can be evaluated explicitly for the symmetric two-channel model illustrated in Fig. 1(a), giving

$$H(x)=\frac{8\gamma k^2+(1-x)(k^2-k_d^2)k-2\gamma k_d^2(1+x)}{(1-x)k[(2\gamma k+k^2-k_d^2)^2-x(k^2-k_d^2)^2]}, \tag{31}$$

where $k=(k_1+k_2)/2$ and $k_d=(k_1-k_2)/2$. Expansion of the above-given expression in terms of x results in

$$\mathrm{Cor}(n)=\left(\frac{k^2-k_d^2}{k^2-k_d^2+2k\gamma}\right)^{2n}\approx\left(\frac{k}{k+2\gamma}\right)^{2n}, \tag{32}$$

where the approximation is introduced for $k_d\ll k$. In the slow relaxation limit, Eq. (32) reduces to $\mathrm{Cor}(n)\approx\exp(-4\gamma/k)=\exp(-2\gamma t_{\mathrm{eff}})$, which agrees with the memory function for the two-channel model $\chi(t)=\chi(0)\exp(-2\gamma t)$.

B. Slow modulation limit

When conformational kinetics is much slower than reaction kinetics, each event can be approximated by a Poisson

process with a probability to jump from one channel to another. Since the on-time duration measures the rate constant for one event within this approximation, the on-time correlation function directly measures the correlation of the reaction rate. This simple reasoning leads to the following derivation.

For Eq. (7) in Ref. 21, the on-time correlation function $\overline{t_1 t_{n+1}}$ is given by

$$\overline{t_1 t_{n+1}} = \frac{1}{k_a}\left\langle \left[\frac{1}{K_a+\Gamma_a}K_b\frac{1}{K_b+\Gamma_b}K_a\right]^n \frac{1}{K_a+\Gamma_a}\right\rangle, \quad (33)$$

where t_1 and t_{n+1} are the time durations for the two on-time events separated by n off-time events. For simplicity, we consider the case when $\Gamma_a=\Gamma_b=\Gamma$ such that the equilibrium distribution satisfies $\Gamma\rho_a=\Gamma\rho_b=0$. Under this condition, two rate matrices K_a and K_b are proportional to each other[21] and we have $(K_a+\Gamma)^{(-1)}\rho_a=K_a^{(-1)}\rho_a$. Second-order expansion in terms of $\delta K_a=K_a-k_a$ leads to

$$\frac{1}{K_a+\Gamma} = \frac{1}{k_a+\Gamma+\delta K_a} \approx \frac{1}{k_a+\Gamma}\left(1-\delta K_a\frac{1}{k_a+\Gamma}+\delta K_a\frac{1}{k_a+\Gamma}\,\delta K_a\frac{1}{k_a+\Gamma}\right) \quad (34)$$

and a similar expression for $K_a(K_a+\Gamma)^{(-1)}$. In the slow modulation limit, when the eigenvalues of Γ are much smaller than k_a, Eq. (33) can be evaluated with above-given approximations to give

$$\begin{aligned}\overline{t_1 t_{n+1}} \approx \frac{1}{k_a^2}\Bigg[1+\left\langle\frac{\delta K_a}{k_a}\frac{k_a}{k_a+\Gamma}\frac{\delta K_a}{k_a}\right\rangle &-\left\langle\frac{\delta K_a}{k_a}\frac{k_a}{k_a+\Gamma}\sum_{m=0}^{n-1}\left(\frac{k_b}{k_b+\Gamma}\frac{k_a}{k_a+\Gamma}\right)^m \right.\\ &\left.\times\left(1-\frac{k_b}{k_b+\Gamma}\frac{k_a}{k_a+\Gamma}\right)\frac{\delta K_a}{k_a}\right\rangle\Bigg]\\ \approx \frac{1}{k_a^2}+\frac{1}{k_a^2}&\left\langle\frac{\delta K_a}{k_a}\exp\left[\Gamma\left(\frac{n}{k_a}+\frac{n}{k_b}\right)\right]\frac{\delta K_a}{k_a}\right\rangle, \end{aligned} \quad (35)$$

where $\chi(t)=\langle \delta K_a G(t)\delta K_a\rangle$ is the memory function for rate fluctuations, and only the leading order correlation of δK is retained approximately. Thus, the cross-correlation function of two on-time events separated by n off-time events is related to $\chi(t)$ as

$$\mathrm{Cor}(n)=\frac{\overline{t_1 t_{n+1}}-\overline{t}^{\,2}}{\overline{t^2}-\overline{t}^{\,2}}=\frac{\chi(t_{\mathrm{eff}})}{\chi(0)} \quad (36)$$

with $t_{\mathrm{eff}}=n/k_a+n/k_b$. In conclusion, in the slow modulation limit, the on-time correlation function is proportional to the memory function of rate fluctuations due to conformational dynamics.

C. Examples

As a numerical example, we study the linear three-channel model illustrated in Fig. 1(b) with

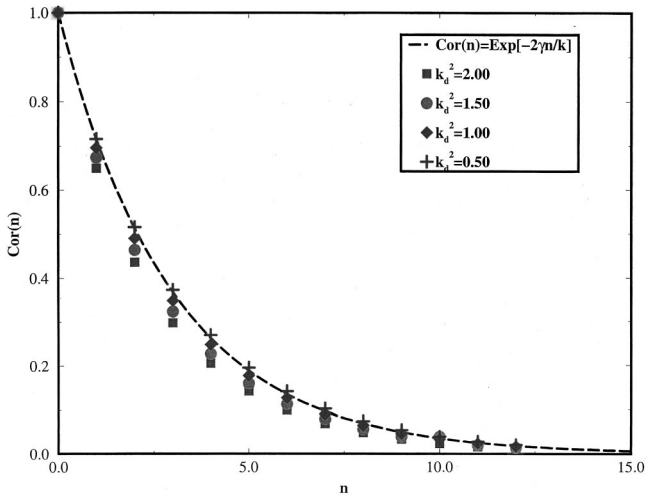

FIG. 6. A comparison of the on-time correlation function Cor(n) with the normalized memory function for the linear three-channel model, $\exp(-2\gamma n/k)$, for several values of rate variance $\chi(0)=k_d^2$. The three-channel model is defined in Eq. (37) with $k=3.0$, $\eta=1.0$, and $\gamma=0.5$.

$$\Gamma_a=\Gamma_b=\begin{pmatrix}\gamma & -\gamma & 0\\ -\gamma & 2\gamma & -\gamma\\ 0 & -\gamma & \gamma\end{pmatrix},$$
$$K_a=\eta K_b=\begin{pmatrix}k+\sqrt{3/2}k_d & 0 & 0\\ 0 & k & 0\\ 0 & 0 & k-\sqrt{3/2}k_d\end{pmatrix}, \quad (37)$$

which has a memory function $\chi(t)=k_d^2\exp(-\gamma t)$. The conformational dynamics are the same for the two states, and the equilibrium coefficient η is the ratio between the backward and forward rate constants. We first consider a symmetric reaction with $\eta=1.0$. In Fig. 6, Cor(n) is plotted for the three-conformational-channel model defined in Eq. (9) with several values of k_d but with fixed k and γ. Evidently, the equivalence relation is approximately obeyed and the deviation from the theoretical prediction increases with the variance. In Fig. 7, the on-time correlation function is plotted for the same values of k and k_d but for three different values of γ. The agreement between the discrete Cor(n) and the memory function $\exp(-2\gamma n/k)$ is reasonably accurate and improves as γ decreases. As an example of the asymmetric reaction, we take the ratio between the forward and backward rate constants as $\eta=2.0$. The on-time correlation function of the asymmetric linear three-channel model is plotted in Fig. 8 and is compared favorably with the memory function.

V. TWO-EVENT NUMBER DENSITY

Time trajectories in single-molecule experiments provide detailed records of single-molecule events; therefore, statistical analysis of single-molecule trajectories can provide rich information of conformational dynamics. In addition to the on-time correlation function, we introduce here a new single-molecule measurement: the number density of single-molecule sequences. In a special experimental setup, short laser pulses are constantly applied on the reactant at a very

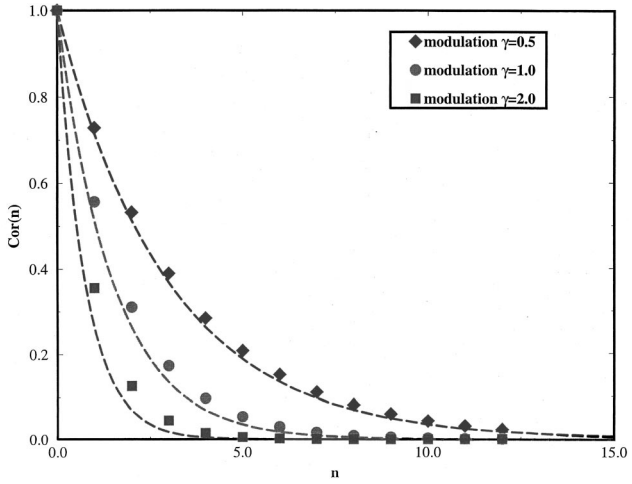

FIG. 7. A plot of the on-time correlation function Cor(n) for the same model as in Fig. 6 for several values of γ, along with the normalized memory function $\exp(-2\gamma n/k)$.

high frequency so that the single reactive system is quickly pumped back to the bright state once oxidized to the dark state. As a result, a trajectory of on events are collected with instantaneous interuptions of dark events. Figure 9 illustrates a typical trajectory with a sequence of length t. The number density of on-time events is the probability distribution function of two events along a single-molecule sequence as a function of their time separation t regardless of the number of events in between. Here, a sequence is defined from the beginning of one event to the end of the same or another event. The two-event number density thus defined will be shown to be proportional to the memory function of the stochastic rate.

The reaction from the bright state to the dark state is denoted by the rate operator K, the conformational dynamics is governed by the operator Γ, and the stationary population distribution satisfies $\Gamma\rho=0$. The number density $N(t)$ with the time duration t is formulated in Laplace space as

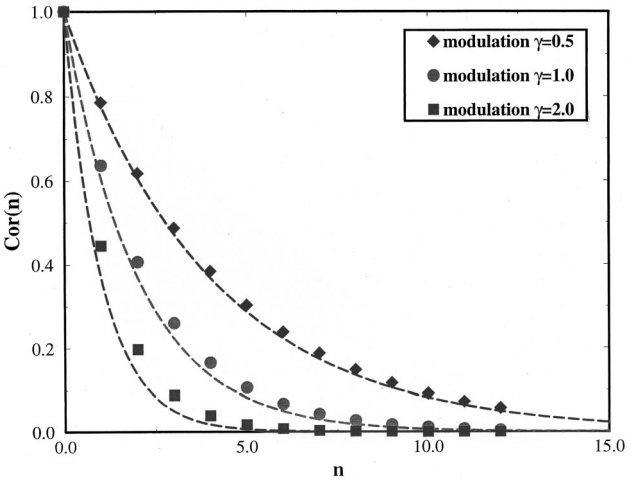

FIG. 8. A comparison of the on-time correlation function Cor(n) with the effective memory function for an asymmetric reaction. The three-channel model is defined in Eq. (37) with the forward rates $k_a=3.0$, the variance $k_d=1/\sqrt{6.0}$, and the equilibrium ratio $\eta=2.0$. The modulation kinetics is the same for both the bright and dark states.

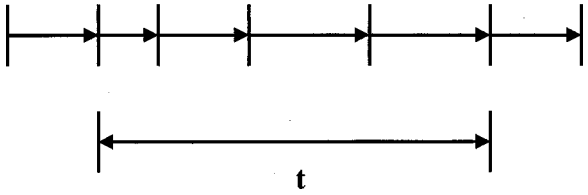

FIG. 9. A sequence of on-events interrupted by instantaneous dark events for the case where the system is constantly pumped back to the bright state.

$$\tilde{N}(u)=\left\langle K\frac{1}{u+K+\Gamma}\left[1-K\frac{1}{u+K+\Gamma}\right]^{-1}K\right\rangle \Big/ k$$
$$=\frac{1}{k}\left\langle K\frac{1}{u+\Gamma}K\right\rangle=k\left[\frac{1}{u}+\frac{1}{k^2}\left\langle \delta K\frac{1}{u+\Gamma}\delta K\right\rangle\right], \tag{38}$$

where $k=\langle K\rangle$ is the average rate and $\delta K=K-k$ is the fluctuation of the rate. Thus, in the time domain, we have

$$N(t)=k\left[1+\frac{1}{k^2}\chi(t)\right], \tag{39}$$

where $\chi(t)=\langle \delta K\exp[-\Gamma t]\delta K\rangle$ is the memory function of the stochastic rate. It is important to note that the above-given relation is obtained without any approximation and thus provides an exact relation between the two-event number density $N(t)$ and the memory function $\chi(t)$ under this experimental setup. A related but approximate relation is discussed in Appendix C.

Similar quantities are defined in single-molecule experiments with both on and off times, as illustrated in Fig. 10. For simplicity, we consider the case with the same conformational dynamics for both bright and dark states, and assume detailed balance condition $\Gamma\rho_a=\Gamma\rho_b=0$. Under this condition, K_a and K_b must be proportional to each other in order to exclude nonstationary effects or net current among different conformational channels. Then, $N_{aa}(t)$ in Laplace space is

$$\tilde{N}_{aa}(u)=\frac{1}{k_a}\left\langle K_a\frac{1}{u+K_a+\Gamma}\right.$$
$$\left.\times\left[1-K_b\frac{1}{u+K_b+\Gamma}K_a\frac{1}{u+K_a+\Gamma}\right]^{-1}K_a\right\rangle$$
$$=\langle K_a(u+K_a+K_b+\Gamma)^{-1}(u+K_b+\Gamma)$$
$$\times(u+\Gamma)^{-1}K_a\rangle/k_a, \tag{40}$$

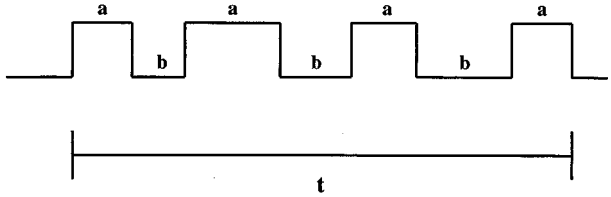

FIG. 10. A sequence of on–off events with length t that starts and ends with on-time events along a typical single-molecule trajectory.

where $k_a=\langle K_a\rangle$ and $k_b=\langle K_b\rangle$ are the average forward and backward rates. In the slow modulation limit, when the characteristic time in Γ is much greater than $1/k_a$ and $1/k_b$, we have

$$[u+K_a+K_b+\Gamma]^{-1}(u+K_b+\Gamma)\approx\begin{cases}k_b/(k_a+k_b) & \text{when } u\ll k_a,k_b\\ (u+K_a+K_b)^{-1}(u+K_b) & \text{when } u\gg k_a,k_b,\end{cases} \tag{41}$$

where $K_a\propto K_b$ is applied and Γ is ignored due to the separation of conformational and reaction time scales. Combining the above two equations, we have

$$\tilde{N}_{aa}(u)\approx\begin{cases}k_b\langle K_a(u+\Gamma)^{-1}K_a\rangle/[k_a(k_a+k_b)] & \text{when } u\ll k_a,k_b\\ \langle K_a[k_bu^{-1}+k_a(u+K_a+K_b)^{-1}]K_a\rangle/[k_a(k_a+k_b)] & \text{when } u\gg k_a,k_b,\end{cases} \tag{42}$$

or, in the time domain,

$$N_{aa}(t)\approx\begin{cases}\dfrac{k_ak_b}{k_a+k_b}\left[1+\dfrac{1}{k_a^2}\chi_{aa}(t)\right], & k_at,k_bt\gg 1\\ \dfrac{k_b}{k_a(k_a+k_b)}\langle K_aK_a\rangle+\dfrac{1}{k_a+k_b}\langle K_a\exp[-(K_a+K_b)t]K_a\rangle, & k_at,k_bt\ll 1,\end{cases} \tag{43}$$

where $\chi_{aa}(t)=\langle\delta K_a\exp[-\Gamma t]\delta K_a\rangle$ is the memory function of the stochastic rate.

The central result of this section, Eqs. (40) and (43), leads to several observations:

(1) In a Poisson process, there is no memory, i.e., $\chi(t)=0$ and $\delta K_a=\delta K_b=0$, the number density $N_{aa}(t)$ is given by the Eq. (43) as

$$N_{aa}(t)=\frac{k_ak_b}{k_a+k_b}+\frac{k_a^2}{k_a+k_b}\exp[-(k_a+k_b)t], \tag{44}$$

which decays to the constant plateau $k_ak_b/(k_a+k_b)$ in the long time limit.

(2) With a separation of time scales implied by the slow modulation condition, the initial fast decay of the number density is followed by the slow decay. The plateau value of the slow decay in the number density is the constant for the Poisson process: $\lim_{t\to\infty}N_{aa}(t)=k_ak_b/(k_a+k_b)$. Hence, the slow decay to this constant allows us to map out the memory function

$$\frac{N_{aa}(t)-N_{aa}(\infty)}{N_{aa}(\infty)}\approx\frac{\chi_{aa}(t)}{k_a^2}, \tag{45}$$

which is more accurate than the on-time correlation function.

(3) In the short time limit, the rate fluctuates on a time scale much greater than the measurement time t under the slow modulation condition so that each reaction channel evolves independently. As a result, the short time limit in Eq. (43) is equivalent to the inhomogenous evarage of the number density associated with each reaction channel.

(4) In the limit of $k_b\to\infty$, $N_{aa}(t)\to k_a[1+\chi_{aa}(t)/k_a^2]$ recovers exactly the previous result in Eq. (39) when laser pulses constantly pump the single molecule from the dark state back to the bright state.

Following the same derivation, $N_{bb}(t)$, $N_{ba}(t)$, and $N_{ab}(t)$ can be obtained as

$$N_{bb}(t)\approx\begin{cases}\dfrac{k_ak_b}{k_a+k_b}\left[1+\dfrac{1}{k_b^2}\chi_{bb}(t)\right], & k_at,k_bt\gg 1\\ \dfrac{k_a}{k_b(k_a+k_b)}(\langle K_bK_b\rangle+\langle K_b\exp[-(K_a+K_b)t]K_b\rangle), & k_at,k_bt\ll 1,\end{cases} \tag{46}$$

$$N_{ab}(t)\approx\begin{cases}\dfrac{k_ak_b}{k_a+k_b}\left[1+\dfrac{1}{k_ak_b}\chi_{ab}(t)\right], & k_at,k_bt\gg 1\\ \dfrac{1}{k_a+k_b}(\langle K_aK_b\rangle-\langle K_a\exp[-(K_a+K_b)t]K_b\rangle), & k_at,k_bt\ll 1.\end{cases} \tag{47}$$

Note that $N_{ab}(t)=N_{ba}(t)$ reflects the time reversal symmetry in the counting. From Eq. (47), the short time limit of $N_{ab}(t)$ equals zero, which is due to the zero probability for finding a zero length duration starting with an on-time event and ending with an off-time event. In contrast, the initial value of the on–on number density is $N_{aa}(0)=\langle K_a^2\rangle/k_a$, which is proportional to the mean square of the forward rate.

As a numerical example, we calculate the quantities $N_{aa}(t)$ and $\chi_{aa}(t)$ for the linear three-channel model as we used for Cor(n) with $K_b=\eta K_a$. Under these parameters, the memory function $\chi_{aa}(t)/k_a^2=k_d^2\exp(-\gamma t)/k^2$, and $k_ak_b/(k_a+k_b)=\eta k/(\eta+1)$. The approximate expression in Eq. (43) and the exact expression in Eq. (40) are calculated and compared in Fig. 11(a) for the short time regime and in Fig. 11(b) for the long time regime, respectively. As shown in the figures, $N_{aa}(t)$ calculated with Eq. (40) decays sharply within a short time scale. The initial value of $N_{aa}(t)$ can be deduced from Eq. (43) in the limit $t\to 0$, giving $N_{aa}(t\to 0)=\langle K_bK_b\rangle/k_b=\eta k(1+k_d^2/k^2)$, which agrees well with the calculated value. The predictions from Eq. (43) fit the curve of the $N_{aa}(t)$ from Eq. (40) over a wide range of time scales.

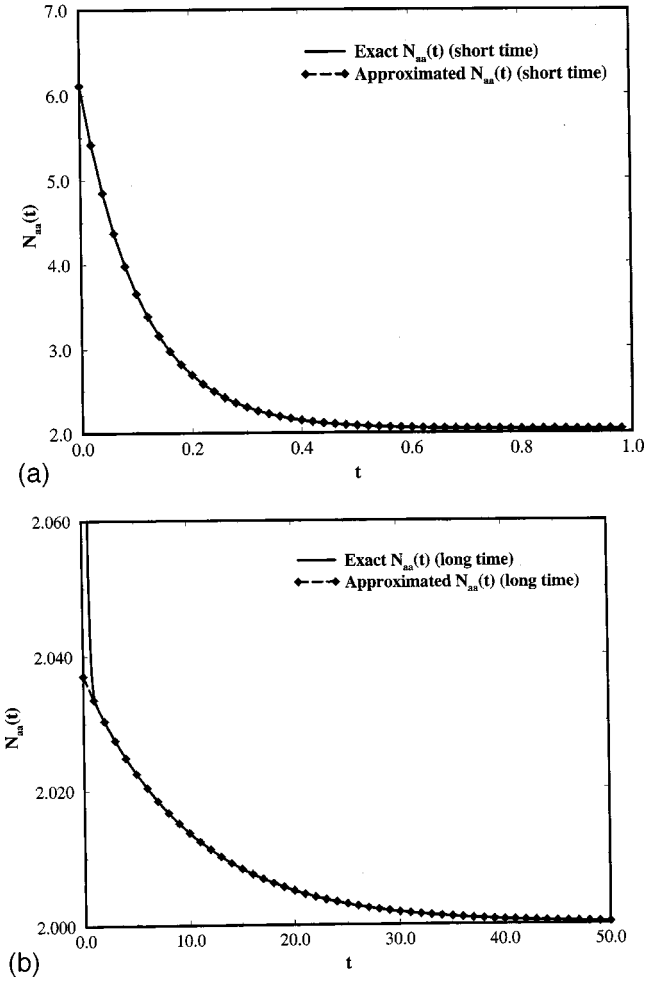

FIG. 11. Comparison between $N_{aa}(t)$ from Eqs. (40) and (43) for a linear three-channel reaction with $k=3.0$, $k_d=1/\sqrt{6}$, $\gamma=0.1$, and $\eta=2.0$. (a) The short-time approximation $N_{aa}(t)$ given in Eq. (43) agrees well with the result calculated from Eq. (40) in the short time regime. (b) The long-time approximation $N_{aa}(t)$ given in Eq. (43) agrees with the result from Eq. (40) over a wide range of time scales except for the short short time period.

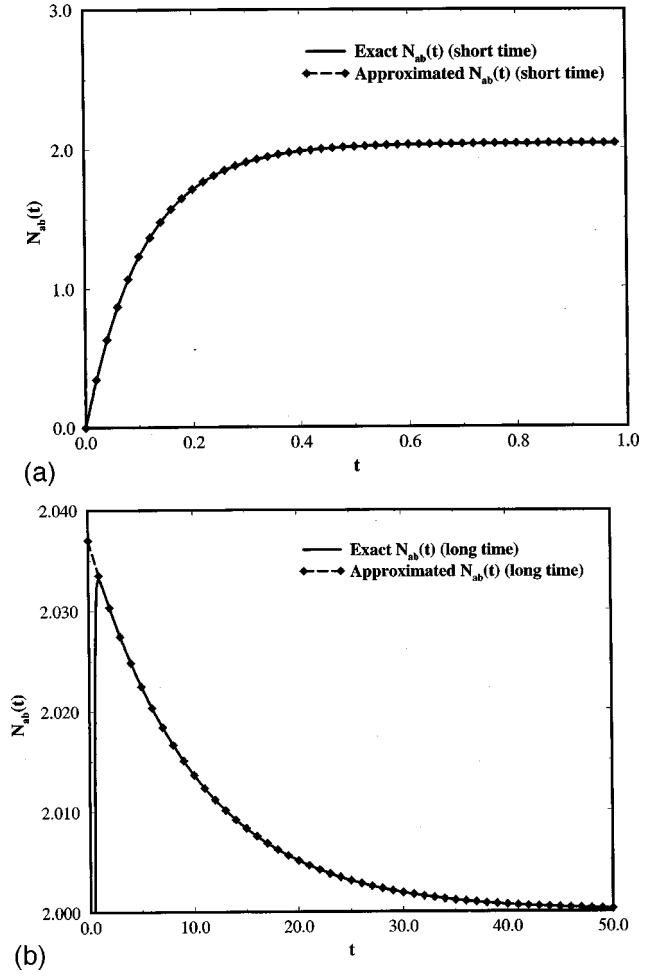

FIG. 12. Density probability distribution function of on–off sequence $N_{ab}(t)$ for the same model used in Fig. 11. (a) The short-time approximation $N_{ab}(t)$ given in Eq. (47) agrees well with the exact result in the short time regime. (b) The long-time approximation $N_{ab}(t)$ given in Eq. (47) agrees with the exact result over a wide range of time scales except for the short short time period.

Similar observation can be made for $N_{ab}(t)$ in Fig. 12, which has a zero initial value. The only difference is that the initial value of N_{ab} is zero, because the on–off sequence involves at least one on event and one off event.

VI. CONCLUSION

In summary, we have rigorously established the stochastic rate approach in the interaction representation of the modulated reaction model. The cross correlation of the stochastic rate defines the memory function and characterizes the rate process. The memory function can be decomposed into the normal modes of conformational fluctuations and directly probes the fundamental mode of environments in the long time limit.

Within this formalism, we study two direct single-molecule measurements of the memory function of the fluctuating rate. The correlation of two on-time events separated by a given number of off events is shown to be proportional to the memory function evaluated at the discretized average time separation between the two on-time events. The relaxation to the asympototic value of the two-event number den-

sity is shown to be proportional to the memory function, thus allowing us to obtain the memory function over the complete time domain except for the initial time. The on-time correlation function has been used in analyzing single-molecule data, whereas the number density proposed here is a new quantity that has not been used yet. The same formalism also leads to the explicit derivation of the echo in the two-event joint probability distribution function (see Appendix A). The three complementary measurements (two-event echo, on-time correlation, and number density) are experimentally feasible and will help to quantify conformational dynamics in single-molecule kinetics.

ACKNOWLEDGMENTS

This research is supported by the AT&T Research Fund Award and the NSF Career Award. We thank Barkai, Sung, Xie and his group for discussions and suggestions.

APPENDIX A: FRET MEASUREMENTS OF CONFORMATIONAL KINETICS

The fine time resolution of single-molecule fluorescence resonant energy transfer (FRET) leads to snapshots of conformation kinetics. To see this point, we write the survival probability as

$$S(t)=\int dr_0 \exp[-(\Gamma+K)t]\rho(r_0)$$
$$=\int dr_0 \left\langle \exp\left[-\int_0^t K(\tau)d\tau\right]\right\rangle_0 \rho(r_0), \tag{A1}$$

where r_0 represents the initial conformational configuration and the average is a conditional average for a given initial condition. Here, K governs the decay lifetime used to probe conformational kinetics and depends on conformational configurations as $k(r)$. Depending on the probing process, $k(r)$ can be the energy transfer rate or the electron transfer rate. In the second expression, $K(\tau)=k[r(\tau)]$ is determined by the conformational trajectory starting from the initial condition r_0. To first order in cumulant expansion, we have

$$S(t)\approx \int dr_0 \exp\left[-\int_0^t \langle k[r(\tau)]\rangle_0 d\tau\right]\rho(r_0), \tag{A2}$$

where $\langle k[r(\tau)]\rangle_0$ is the average of all conformational trajectories starting from r_0. Let us assume that the conformational coordinate follows Gaussian dynamics $\langle r(t)\rangle=0$ and $\langle r(t)r(0)\rangle=\langle r^2\rangle\phi(t)$. Then, the average rate at time t in Eq. (A2) is given by

$$\langle k[r(\tau)]\rangle_0=\frac{1}{\sqrt{2\pi\Delta}}\int d\xi k[r_0\phi(t)+\xi]\exp[-\xi^2/2\Delta], \tag{A3}$$

where ξ is the Gaussian variable and $\Delta=\langle r^2\rangle[1-\phi^2(t)]$ is the Gaussian width. Evidently, if the decay rate is much faster than the conformational relaxation time scale, we approximately write $S(t)=\int \rho(r_0)\exp[-tk(r_0)]dr_0$, which is an inhomogeneous average of the equilibrium distribution. In this case, we obtain both fine time and spatial resolution. If the decay rate is slow in comparison to conformational coordinates, then the trajectory average in Eq. (A2) reduces the spatial resolution while still maintaining the temporal resolution.

We now consider the correlation of two lifetimes separated by time t. Assuming the fast decay limit, we write the lifetime correlation function as

$$\mathrm{Cor}(t)=\left\langle \delta\frac{1}{K}\exp(-\Gamma t)\delta\frac{1}{K}\right\rangle \Big/ \left\langle\left(\delta\frac{1}{K}\right)^2\right\rangle, \tag{A4}$$

where the ensemble average is defined for the equilibrium conformation distribution. If the variance of the rate δK is much smaller than the average rate $\langle k\rangle$, we have

$$\mathrm{Cor}(t)\approx\frac{\langle \delta K\exp(-\Gamma t)\delta K\rangle}{\langle \delta K^2\rangle}=\frac{\chi(t)}{\chi(0)}, \tag{A5}$$

where the memory function $\chi(t)$ is defined similarly as in Eq. (11). Evidently, the general relation between the on-time correlation function and the memory function remains valid for the simpler case discussed in this appendix.

APPENDIX B: TWO-EVENT JOINT PROBABILITY DISTRIBUTION FUNCTION

The two-event echo was explored extensively in a recent publication, where an expression for the echo is obtained through the Gaussian approximation.[21] However, the Gaussian rate model is determined by mapping the survival probability computed from the modulated reaction model. The rigorous definition of the stochastic rate in Sec. III quantifies the mapping and allows us to establish the two-event echo phenomena in a broad context.

Without loss of generality, our analysis is carried out for symmetric reactions with $\Gamma_a=\Gamma_b=\Gamma$ and $K_a=K_b=K$. Numerical calculations of the asymmetric reaction in Sec. IV suggest that the conclusions drawn for symmetric reactions hold for asymmetric reactions. The symmetric reaction can be understood as the limiting case of fast backward rate processes. Applying the Gaussian stochastic approximation to symmetric reactions, we obtain the single-event distribution function

$$kf(t)=\langle K\exp(-Kt-\Gamma t)K\rangle$$
$$\approx\{[k-L(t)]^2+\chi(t)\}\exp[-kt+M(t)] \tag{B1}$$

and the joint distribution function for adjacent on–off events

$$kf(t_1,t_2)=\langle K\exp(-Kt_1-\Gamma t_1)K\exp(-Kt_2-\Gamma t_2)K\rangle$$
$$\approx\{[\chi(t_1)+\chi(t_2)][k-L(t_1+t_2)]$$
$$+[k-L(t_1)-L(t_2)]\chi(t_1+t_2)$$
$$+[k-L(t_1+t_2)]^2[k-L(t_1)-L(t_2)]\}$$
$$\times\exp[-k(t_1+t_2)+M(t_1+t_2)], \tag{B2}$$

where $L(t)=\int_0^t\chi(\tau)d\tau$. Under the small variance condition, the difference function $\delta(t_1,t_2)=f(t_1,t_2)-f(t_1)f(t_2)$ is approximated by

$$\delta(t_1,t_2)\approx\chi(0)\exp[-k(t_1+t_2)]\{\chi(t_1+t_2)+k[L(t_1)+L(t_2)-2L(t_1+t_2)]-k^2[M(t_1)+M(t_2)-M(t_1+t_2)]\}, \tag{B3}$$

which is in the linear order of $\chi(0)$. For further analysis, we assume a single exponential decay form, $\chi(t)=\chi(0)\times\exp(-\lambda t)$, so that

$$\delta(t_1,t_2)\approx\chi(0)\frac{\exp[-(k+\lambda)(t_1+t_2)]}{\lambda^2}(k+\lambda-ke^{2\lambda t_1})\times(k+\lambda-ke^{2\lambda t_2}). \tag{B4}$$

Then, the difference function has a maximum at the echo time

$$t_e=\frac{2}{\lambda}\ln\frac{k+\lambda}{k}, \tag{B5}$$

and a minimum at the focal time, which is half the echo time, $2t_f=t_e$. The difference function also has a minimum along the t_1 axis and the t_2 axis at the focal time t_e. The small variance expansion implies that the echo amplitude is proportional to the variance of the reaction rate. These features have been confirmed in Ref. 21 with an extensive calculation of multiple channel models and the continuous diffusion controlled reaction model. The prediction of the focal time in the single-event distribution function and of the recurrent behavior in the two-event distribution function helps reveal the nature of conformational landscapes. Similar to the photon echo phenomenon, the recurrence can be understood as the echo signal due to the inhomogeneous distribution of environments, and the conformational modulation can be understood as dephasing.[21] Analogous to motional narrowing, in the fast modulation limit, the echo signal vanishes, and the single exponential law is recovered. The height of the echo signal and its position vary with the modulation rate and can be a sensitive probe of the dynamics disorder resulting from conformational fluctuations.

APPENDIX C: ON-TIME CORRELATION FUNCTION AS A FUNCTION OF TEMPORAL SEPARATION

The moments of on-time events associated with number counting also provide a direct measure of the correlation function of the stochastic rate. As an example, we consider the experimental setup where laser pumping from dark states is constantly applied. In the ensemble of sequences with length t, as shown in Fig. 9, the joint distribution function of the first and last on-time events can be expressed as

$$f(t_1,t,t_2)=[k_sN(t)]^{-1}\left\langle\sum_{n=0}^{\infty}KG(t_2)\times\int dt_1\cdots\int dt_nKG(t-t_1-\cdots-t_n)KG(t_1)\cdots KG(t_n)KG(t_1)K\right\rangle, \tag{C1}$$

where $G(t)=\exp[-(K+\Gamma)t]$ denotes the evolution of a single on-time event and $N(t)$ is the number density of such sequences. In this ensemble of these sequences, the average on-time of the first event is given as

$$\overline{t_2}(t)=\int_0^{\infty}dt_1\int_0^{\infty}t_2dt_2f(t_1,t,t_2)\approx\frac{1}{N(t)}+\mathcal{O}\left(\frac{|\Gamma|}{k_s}\right)\frac{\chi(t)}{k_s^2}, \tag{C2}$$

where $1/|\Gamma|$ is defined as the slowest time scale of the conformation dynamics and the small variance of rate fluctuations is assumed in the calculation. So $\overline{t_2}(t)$ is approximately $1/N(t)$ to the zeroth order of the slow modulation limit when $|\Gamma|\ll k_s$, and $\overline{t_1}(t)$ can be shown as the same. The cross moment of these two on-time events is

$$\overline{t_1t_2}(t)=\int_0^{\infty}t_1dt_1\int_0^{\infty}t_2dt_2f(t_1,t,t_2)\approx\frac{1}{k_sN(t)}+\mathcal{O}\left(\frac{|\Gamma|}{k_s}\right)^2\frac{\chi(t)}{k_s^2}, \tag{C3}$$

so that $\overline{t_1t_2}(t)\approx 1/k_sN(t)$ to the zeroth order of $|\Gamma|/k_s$. Applying the expression of the number density of such sequences $N(t)$ in Eq. (39), the correlation between these two on-time events $\mathrm{Cor}(t)$ is

$$\mathrm{Cor}(t)=\frac{\overline{t_1t_2}(t)-\overline{t_1}(t)\overline{t_2}(t)}{\overline{t_1t_2}(0)-\overline{t_1}(0)\overline{t_2}(0)}=\frac{1/[k_sN(t)]-[1/N(t)]^2}{1/[k_sN(0)]-[1/N(0)]^2}\approx\chi(t)/k_s^4, \tag{C4}$$

which provides another way to measure the memory function of the stochastic rate. The correlation function $\mathrm{Cor}(t)$ defined here is different from the $\mathrm{Cor}(n)$ discussed in Sec. IV. First, $\mathrm{Cor}(n)$ is a disrectized function of the number of events while $\mathrm{Cor}(t)$ is a continuous function of time. Second, $\mathrm{Cor}(n)$ is an event-averaged quantity, which is averaged over all time separations with a given number of intermediate events. Evidently, $\mathrm{Cor}(t)$ and $N(t)$ are mixed average of events and time, whereas the average of $\mathrm{Cor}(t)$ is performed over all the sequences with length t.

[1] T. Bache, W. E. Moerner, M. Orrit, and U. P. Wild, *Single-molecule Optical Detection, Imaging and Spectroscopy* (VCH, Berlin, 1996).
[2] X. S. Xie and J. K. Trautman, Annu. Rev. Phys. Chem. **49**, 441 (1998).
[3] W. E. Moerner and M. Orrit, Science **283**, 1670 (1999).
[4] L. Edman, U. Mets, and R. Rigler, Proc. Natl. Acad. Sci. U.S.A. **93**, 6710 (1996).
[5] Y. Jia, A. Sytnik, L. Li, S. Vladimirov, B. S. Cooperman, and R. M. Hochstrasser, Proc. Natl. Acad. Sci. U.S.A. **94**, 7932 (1997).
[6] T. Ha, A. Y. Ting, J. Liang, A. A. Deniz, D. S. Chemla, P. G. Schultz, and S. Weiss, Chem. Phys. **247**, 107 (1999).
[7] C. G. Baumann, V. A. Bloomfield, S. B. Smith, C. Bustanmante, M. D. Wang, and S. M. Block, Biophys. J. **78**, 1965 (2000).
[8] P. Reilly and J. L. Skinner, Phys. Rev. Lett. **71**, 4257 (1993).
[9] F. L. H. Brown and R. J. Silbey, J. Chem. Phys. **108**, 7434 (1998).
[10] E. Geva and J. L. Skinner, Chem. Phys. Lett. **288**, 225 (1998).
[11] K. Weston, P. J. Carson, H. Metiu, and S. K. Buratto, J. Chem. Phys. **109**, 7474 (1998).
[12] J. Wang and P. Wolynes, J. Phys. Chem. **100**, 1129 (1996).
[13] J. N. Onuchic, J. Wang, and P. G. Wolynes, Chem. Phys. **247**, 89 (1999).

[14] V. Chernyak, M. Schuls, and S. Mukamel, J. Chem. Phys. **111**, 7416 (1999).
[15] E. Barkai, Y. Jung, and R. Silbey, Phys. Rev. Lett. **87**, 207403 (2001).
[16] H. P. Lu, L. Xun, and X. S. Xie, Science **282**, 1877 (1998).
[17] G. K. Schenter, H. P. Lu, and X. S. Xie, J. Phys. Chem. A **103**, 10499 (1999).
[18] J. Cao, Chem. Phys. Lett. **327**, 38 (2000).
[19] N. Agmon, J. Phys. Chem. B **104**, 7830 (2000).
[20] G. H. Weiss and J. Masoliver, Physica A **296**, 75 (2001).
[21] S. Yang and J. Cao, J. Phys. Chem. **103**, 0330 (2001).
[22] S. Okazaki, J. Wang, S. A. Schofield, and P. G. Wolynes, Chem. Phys. **222**, 175 (1997).
[23] N. Agmon and J. J. Hopfield, J. Chem. Phys. **79**, 2042 (1983).
[24] R. I. Cukier and J. M. Deutch, Phys. Rev. **177**, 240 (1969).
[25] J. E. Straub, M. Borkovec, and B. J. Berne, J. Chem. Phys. **84**, 1788 (1986).
[26] H. Tang, S. Jang, M. Zhou, and S. A. Rice, J. Chem. Phys. **101**, 8737 (1994).
[27] M. Zhou and S. A. Rice, Int. J. Quantum Chem. **58**, 593 (1996).
[28] E. J. Heller, J. Phys. Chem. **99**, 2625 (1995).
[29] P. Pechukas and J. Ankerhold, J. Chem. Phys. **107**, 2444 (1997).
[30] R. Kubo, N. Toda, and N. Hashitsume, *Statistical Physics II* (Springer-Verlag, Berlin, 1985).
[31] S. Mukamel, *The Principles of Nonlinear Optical Spectroscopy* (Oxford University Press, London, 1995).
[32] J. Wang and P. Wolynes, Phys. Rev. Lett. **74**, 4317 (1995).
[33] A. M. Berezhkovskii, A. Szabo, and G. H. Weiss, J. Chem. Phys. **110**, 9145 (1999).
[34] D. Makarov and H. Metiu, J. Chem. Phys. **111**, 10126 (1999).
[35] J. Cao, J. Chem. Phys. **114**, 5137 (2001).
[36] R. M. Dickson, D. J. Norris, Y. L. Tzeng, and W. E. Moerner, Science **274**, 966 (1996).
[37] G. J. Schutz, H. Schindler, and T. Schmidt, Biophys. J. **73**, 1073 (1997).
[38] X. Xu and E. S. Yeung, Science **275**, 1106 (1997).
[39] T. Ha, J. Glass, T. Enderle, D. S. Chemla, and S. Weiss, Phys. Rev. Lett. **80**, 2093 (1998).
[40] M. A. Osborne, S. Balasubramanian, W. S. Futey, and D. Klenerman, J. Phys. Chem. B **102**, 3160 (1998).
[41] J. Cao, Phys. Rev. E **63**, 041101 (2001).
[42] R. Zwanzig, Acc. Chem. Res. **23**, 148 (1990).
[43] H. Yang, P. Karnchanaphanurach, and X. Xie (preprint).
[44] R. Metzler, E. Barkai, and J. Klafter, Phys. Rev. Lett. **82**, 3563 (1999).